

SEISMIC POWER GENERATOR USING HIGH-PERFORMANCE POLYMER ELECTRET

Takumi Tsutsumino¹, Yuji Suzuki¹, Nobuhide Kasagi¹, and Yoshihiko Sakane²

¹Department of Mechanical Engineering, The University of Tokyo, Japan

²Asahi Glass Corporation, Ltd., Japan

ABSTRACT

Development of a micro electret generator prototype for energy harvesting applications is presented. MEMS-friendly perfluoropolymer, CYTOP is adopted as high-performance electret material. When corona charging is employed, charge density as large as 1.37 mC/m² is obtained for a 15 μm-thick CYTOP film, which is much larger than that of Teflon AF. In power generation experiments using a prototype seismic generator, maximum output power of 38 μW is obtained with 2 mm_{p-p} oscillation at 20 Hz.

1. INTRODUCTION

In the last decade, micro power generation systems that could replace conventional secondary batteries have received significant attention. For low-power consumption applications such as RFIDs and mobile sensor networks, vibration-driven energy harvesting devices are proposed [1, 2]. Since the frequency range of vibration existing in the environment is below a few tens of Hz, electret power generators [3] should have higher performance than electromagnetic ones. Boland et al. [4] developed the first MEMS rotary electret generator and obtained 15 μW power output at 6,000 rpm. Since then, various studies have been made for micro electret power generator [5-8]. However, conventional electret materials such as SiO₂ and Teflon AF are employed in their studies, and the power output obtained with their prototypes remains small.

We recently find that CYTOP (Asahi Glass Co., Ltd.), which is MEMS-compatible amorphous perfluoropolymer, can also be employed as an electret material [7]. In the present study, we develop a prototype micro seismic generator with CYTOP electret, and make a series of power generation experiments.

2. ELECTRET POWER GENERATOR

Figure 1 shows a schematic of the micro electret generator designed in the present study. In seismic operation, the amount of the induced charge on the counter electrode is charged due to the change in the overlapping area, producing electric current in the external circuit. The seismic mass is supported by parylene high-aspect-ratio springs [9], which enable large am-

plitude oscillation and low response frequency.

Figure 2 shows a schematic of the simplified generator structure, where σ , d , g , and A are respectively surface charge density, thickness of electret, gap between the electret and the counter electrode, and the overlapping area. Using a simple capacitance model, Boland et al. [4] show that maximum output power P_{MAX} and optimal external load R_{MAX} of the electret power generator can be given as follows:

$$P_{MAX} = \frac{\sigma^2 \cdot \frac{dA(t)}{dt}}{\frac{4\epsilon_0\epsilon_1}{d} \left(\frac{\epsilon_1 g}{\epsilon_2 d} + 1 \right)}, \quad (1)$$

$$R_{MAX} = \frac{1}{\epsilon_0} \frac{dA(t)}{dt} \left(\frac{d}{\epsilon_1} + \frac{g}{\epsilon_2} \right), \quad (2)$$

where ϵ_0 , ϵ_1 and ϵ_2 are respectively the permittivity of vacuum, dielectric constant of the electret material and that of air. Therefore, P_{MAX} is proportional to the surface charge density squared σ^2 , and is increased with increasing the thickness of electret d .

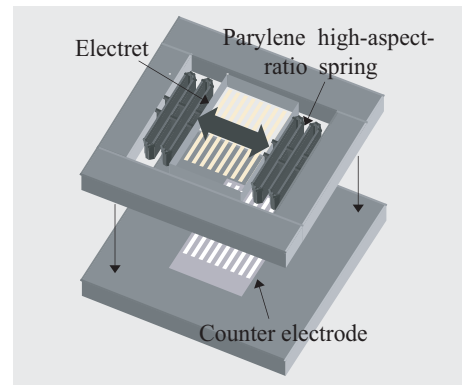


Figure 1. Schematic of the micro electret generator.

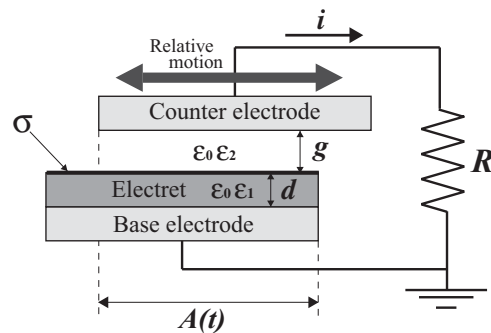


Figure 2. Principle of electret generator.

On the other hand, R_{MAX} is independent of σ , but linearly dependent on d and g . Since P_{MAX} is proportional to the time derivative of the overlapping area $dA(t)/dt$, while R_{MAX} is inversely proportional to $dA(t)/dt$, oscillation frequency, oscillation amplitude, and the number of poles should also have large impact on the generator performance.

Various kinds of materials have been examined for electrets [10]. Among them, dielectric polymer materials, especially perfluoropolymer such as PTFE, are generally employed. Hsieh et al. [11] employ Teflon AF as the electret material for their MEMS microphone. In our previous study [7, 12], we found that CYTOP (CTL-809M, Asahi Glass Co., Ltd.), which is also amorphous perfluoropolymer, can be also used for electrets. We also find that the surface charge density σ for CYTOP is about 3 times larger than that of Teflon AF [12]. As mentioned previously, maximum output power is proportional to σ^2 , so that 9 times larger output power can be expected when CYTOP is employed as the electret material.

Figure 3 shows the time trace of the surface charge density obtained for CYTOP electret. The sample is 15 μm thick, and corona-charged with -8 kV for 30 minutes. The sample keeps high surface charge density of 1.37 mC/m^2 over more than 100 days. Note that CYTOP electret presently fabricated is stable at least up to its glass transition temperature (108 $^\circ\text{C}$) [12].

3. FABRICATION

For power generation experiments, we develop a prototype electret generator. Figure 4 shows the fabrication process of the electret plate. Firstly, Cr/Au/Cr (10/100/10 nm in thickness) thin films are deposited on 0.7 mm-thick Pyrex wafer using an EB evaporator, followed by patterning with standard lithography and wet etching. Then, CYTOP (CTL-809M) is spun-on

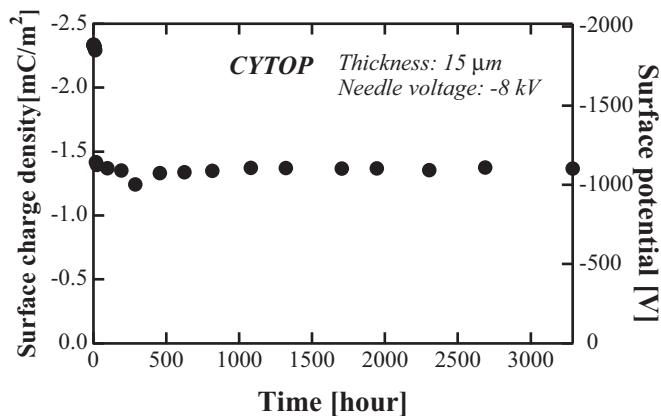


Figure 3. Temporal evolution of surface charge density and surface potential for corona-charged CYTOP electret.

at a rotational speed of 1,000 rpm for 20 seconds and soft-baked at 100 $^\circ\text{C}$ for 30 minutes. This process is repeated 7 times to obtain a 20 μm -thick film, and is fully-cured at 185 $^\circ\text{C}$ for 1.5 hours. As the metal mask of the CYTOP film, copper is evaporated and patterned. Finally, the CYTOP film is etched by O_2 plasma with 100 W RF power for 60-70 minutes. The counter electrode is fabricated with a similar process.

Figure 5 shows the fabricated patterned electret film with guard electrodes. The width of electret and guard electrode is both 1 mm and the gap between them is 30 μm . The total area of the electret is 10 x 20 mm^2 .

After fabrication, the electret plate is charged by corona-charging. The condition of corona-charging is shown in Table 1. The temperature during charging is chosen at a higher temperature than the glass transition one. Average surface voltage of about -1000 V is obtained after charging.

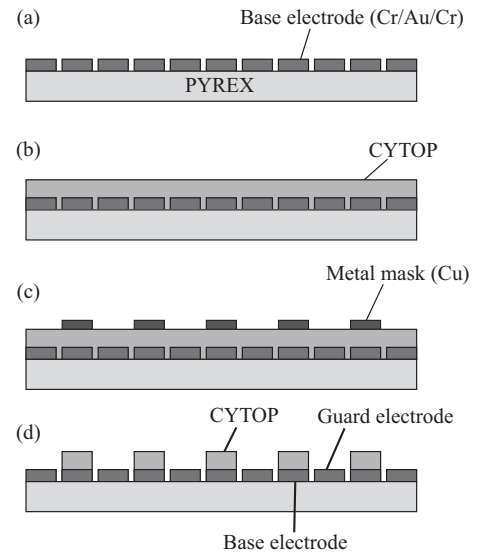


Figure 4. Fabrication process of the electret plate: (a) deposit and pattern base electrode (Cr/Au/Cr), (b) spin-on and cure CYTOP, (c) deposit and pattern metal mask (Cu), (d) O_2 plasma etch and remove metal mask.

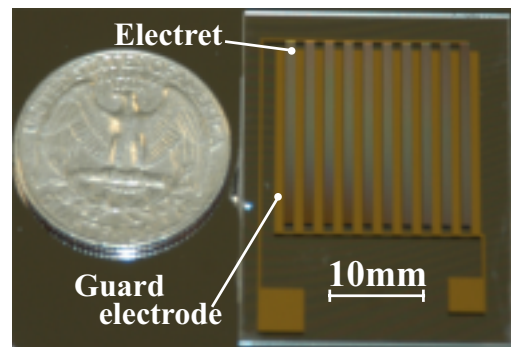


Figure 5. Glass substrate with patterned electret.

Table 1. Condition of corona-charging.

Needle voltage	-8 kV
Grid voltage	-600 V
Temperature	120 °C
Charge time	10 min.

4. POWER GENERATION

Table 2 shows the capacitance between the electret and the counter electrode plates for the gap $g = 100 \mu\text{m}$. Ideally, the capacitance is 17.7 pF for 100 % overlap the electret and the counter electrode, while it is zero for 0 % overlap. It is confirmed that the parasitic capacitance is significantly decreased to 2.3 pF by using the guard electrodes.

The experimental setup for power generation experiment is shown schematically in Fig. 6, which consists of the electret plate, the counter electrode plate, an alignment stage, and an electromagnetic shaker (APS-113, APS Dynamics Inc.). The electret plate and the counter electrode plate are respectively fixed to the shaker and the alignment stage. The gap is measured with a laser displacement meter (LC-2400, Keyence Inc.), and set to 100-200 μm . The counter electrode plate is moved sinusoidally in the horizontal direction by the shaker. In order to measure the output voltage for various external loads, a simple measuring circuit with a voltmeter and two resistances in series is employed.

Firstly, the gap and the oscillation amplitude are respectively set to 200 μm and 1 mm_{p-p}. The oscillation frequency f is changed between 5 and 20 Hz. The surface potential of the electret is about 600 V. Figure 7 shows the output power versus the external load R . Maximum output power of 6.4 μW is obtained at $f = 20 \text{ Hz}$ and $R = 100 \text{ M}\Omega$. At each frequency, the maximum output power and the optimal load are estimated with a curve fit of the experimental data and plotted in Fig. 8. Each quantity is normalized by its value at $f = 5 \text{ Hz}$. It is found that the experimental data are in good agreement with the predicted values using Eqs. (1) and (2); the power output is proportional to f , and the optimal load is inversely proportional to f .

Figure 9 shows the results for a smaller gap of 100 μm . The oscillation amplitude and frequency are respectively set to 2 mm_{p-p} and 20 Hz. The initial surface potential of the electret is about -950 V. Maximum output power of 37.7 μW is obtained at $R = 60 \text{ M}\Omega$. Figure 10 shows the time trace of the output voltage obtained with $R = 60 \text{ M}\Omega$. The output wave pattern is almost sinusoidal and its peak-to-peak voltage is as large as 150 V.

However, the surface potential of the electret after the ex-

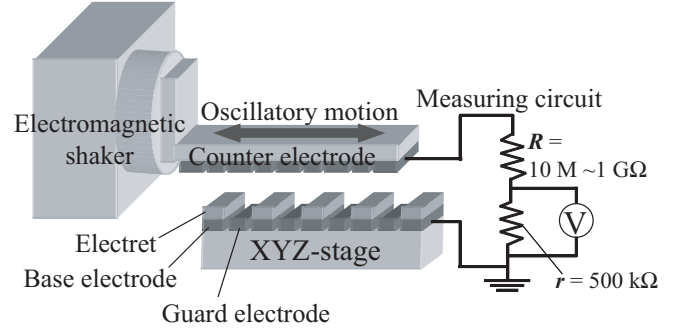


Figure 6. Schematic diagram of the experimental setup for power generation.

Table 2. Variation of capacitance between a patterned electret and a patterned counter electrode.

Overlapping area	Without guard electrodes	With guard electrodes	Theoretical value
	100%	39.8 pF	
0%	25.4 pF	2.3 pF	0.0 pF

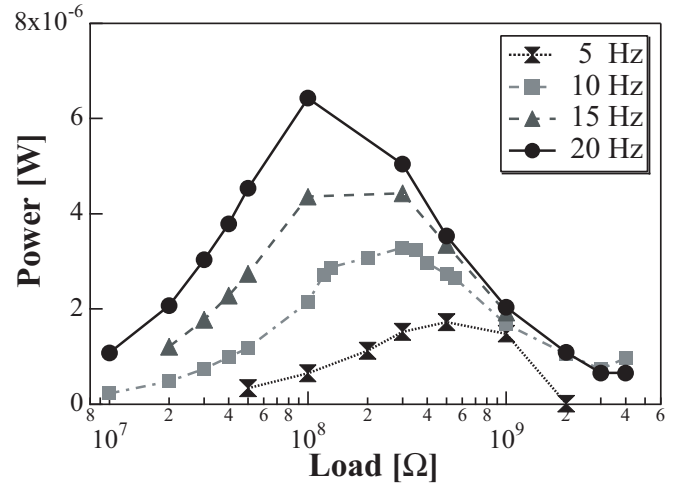


Figure 7. Power output versus external load for $g = 200 \mu\text{m}$.

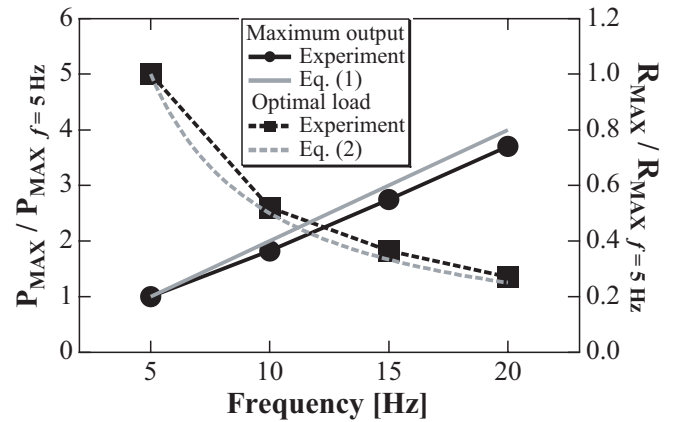


Figure 8. Maximum output power and optimal load versus oscillation frequency for $g = 200 \mu\text{m}$. Each quantity is normalized with its values at $f = 5 \text{ Hz}$.

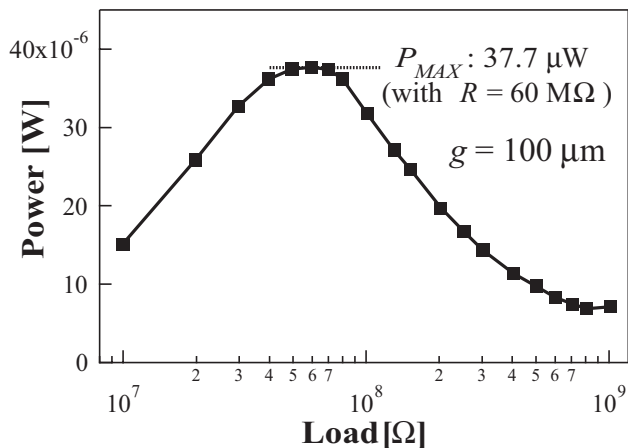


Figure 9. Output power versus external load at $f = 20$ Hz.

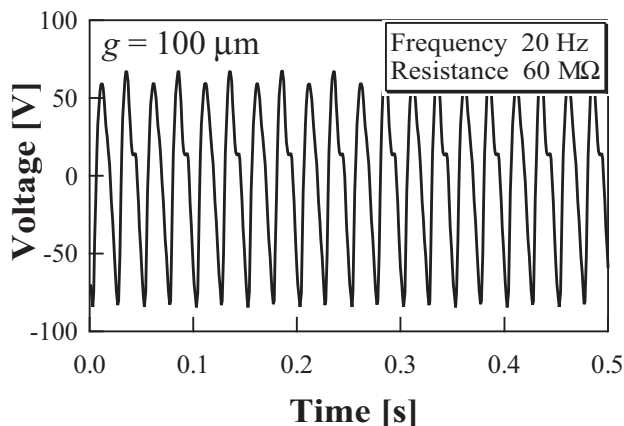


Figure 10. Time trace of the output voltage at $f = 20$ Hz.

periment drops to about -400 V. This should be caused by the electric break down between the electret plate and the counter electrode plate, since the break down voltage of air for a 100 μm gap is about 1000 V. Therefore, the gap should be in vacuum or filled with insulating gas (e.g., SF_6) for experiments for larger output power with smaller gaps. When the gap, the width of electret, and the oscillation amplitude are respectively 50 μm , 200 μm , and 1 mm_{p-p}, output power as large as 1 mW is expected at 20Hz oscillation.

5. CONCLUSION

We develop a MEMS-friendly electret film using CYTOP, and examine its performance with a prototype micro seismic generator. The following conclusions can be derived.

- (1) The stable surface charge density of 1.37 mC/m² is obtained for 15 μm -thick CYTOP.
- (2) The trend of maximum output power and optimal load resistance of a prototype generator is in good accordance with that of theoretical values.
- (3) The maximum output power of 37.7 μW and peak-to-peak voltage of 150 V are obtained at 20 Hz oscillation with 60 M Ω external load.

This work is partially supported through Grant-in-Aid for Scientific Research (B) (No. 17360092) by MEXT, Japan. Photomasks are made using the University of Tokyo VLSI Design and Education Center (VDEC)'s 8-inch EB writer F5112+VD01 donated by ADVANTEST Corporation.

REFERENCE

- [1] C. B. Williams, and R. B. Yates, "Analysis of a Micro-electric Generator for Microsystems," *Sensors and Actuators, A*, Vol. 52, 1996, pp. 8-11.
- [2] S. Roundy, P. K. Wright, and J. Rabaey, "A Study of Low Level Vibration as a Power Source for Wireless Sensor Nodes," *Computer Communication*, Vol. 26, 2003, pp. 1131-1144.
- [3] Y. Tada, "Theoretical Characteristics of Generalized Electret Generator, Using Polymer Film Electrets," *IEEE Trans. Electrical Insulation*, Vol. 21, 1986, pp. 457-464.
- [4] J. Boland, C.-H. Chao, Y. Suzuki, and Y.-C. Tai, "Micro Electret Power Generator," *Proc. 16th IEEE Int. Conf. MEMS*, Kyoto, 2003, pp. 538-541.
- [5] T. Sterken, P. Fiorini, K. Baert, G. Borghs, and R. Puers, "Novel Design And Fabrication of A MEMS Electrostatic Vibration Scavenger," *Proc. PowerMEMS 2004*, Kyoto, 2004, pp. 18-21.
- [6] T. Genda, S. Tanaka, and M. Esashi, "High Power Electret Motor and generator on Shrouded Turbine," *Proc. PowerMEMS 2004*, Kyoto, 2004, pp. 183-186.
- [7] Y. Arakawa, Y. Suzuki, and N. Kasagi, "Micro Seismic Power Generator Using Electret Polymer Film," *Proc. PowerMEMS 2004*, Kyoto, 2004, pp. 187-190.
- [8] J. Boland, J. D. M. Messenger, H. W. Lo, and Y.-C. Tai, "Arrayed Liquid Rotor Electret Power Generator Systems," *Proc. 18th IEEE Int. Conf. MEMS*, Miami, 2005, pp. 618-621.
- [9] Y. Suzuki, and Y.-C. Tai, "Micromachined high-aspect-ratio parylene beam and its application to low-frequency seismometer," *Proc. 16th IEEE Int. Conf. MEMS*, Kyoto, 2003, pp. 486-489.
- [10] G. M. Sessler, *Electrets 3rd Edition*, Laplacian Press, 1998.
- [11] W. H. Hsieh, T. J. Yao, and Y.-C. Tai, "A High Performance MEMS Thin-film Teflon Electret Microphone," *Int. Conf. Solid-state Sensors Actuators (Transducers' 99)*, Sendai, 1999, pp. 1064-1067.
- [12] T. Tsutsumino, Y. Suzuki, N. Kasagi, and Y. Tsurumi, "High-Performance Polymer Electret for Micro Seismic Generator," *Proc. PowerMEMS 2005*, Tokyo, 2005, to be presented.